2014 IEEE International Conference on Robotics & Automation (ICRA)
Hong Kong Convention and Exhibition Center
May 31 - June 7, 2014. Hong Kong, China

Visibility Analysis for Autonomous Vehicle Comfortable Navigation

Yoichi Morales, Jani Even, Nagasrikanth Kallakuri, Tetsushi Ikeda, Kazuhiko Shinozawa,
Tadahisa Kondo and Norihiro Hagita
Intelligent Robotics and Communication Laboratories
Advanced Telecommunications Research Institute International

***Abstract*— This work introduces a 3*D* visibility model for comfortable autonomous vehicles. The model computes a visibility index based on the pose of the wheelchair within the environment. We correlate this index with human navigational comfort (discomfort) and we discuss the importance of modeling visibility to improve human riding comfort. The proposed approach models the 3*D* visual field of view combined with a two-layered environmental representation. The field of view is modeled with information from the pose of the robot, a 3*D* laser sensor and a two-layered environmental representation composed of a 3*D* geometric map with traversale area information. Human navigational discomfort was extracted from participants riding the autonomous wheelchair. Results show that there is fair correlation between poor visibility locations (e.g., blind corners) and human discomfort. The approach can model places with identical traversable characteristics but different visibility and it differentiates visibility characteristics according to traveling direction.**

I. Introduction

In human navigation, the walking style (e.g., position within a corridor and velocity) while following a path is influenced by the traversable characteristics of the environment and the good/poor visibility at a certain pose. In the case of blind corners, people tend to slow down and smoothly overshoot while turning as they do not know what to expect on the other side. In the case of a corner with same geometric characteristics but with good visibility, people do not need to slow down nor to overshoot on turns. Figure 1 shows and example of two corners in an environment which present the same geometric traversable configurations, however, because of their composition, the visibility is quite different. The left side of Figure 1, shows an example of a corner with good visibility, therefore, the person on the wheelchair knows what to expect around the corner. In the right image in Figure 1, because of poor visibility, the person on the wheelchair does not know what to expect around the corner. In the latter case, even if no obstacle is present, the wheelchair driver would be careful to slow down in case that evasive action would need to be taken.

This paper points out the importance of modeling the visibility of an environment for comfortable navigation on a passenger vehicle. We discuss the relation between good/poor visibility conditions while driving a wheelchair, we present a model of environment visibility and discuss its importance towards computation of human comfortable trajectories. The visibility analysis is implemented using 3*D* range information from a laser sensor and a two-layered environmental representation.

This research was supported by the Ministry of Internal Affairs and Communications with a contract entitled 'Novel and innovative R&D making use of brain structures." All the authors are with the Advanced Telecommunications Research Institute International, Kyoto, Japan

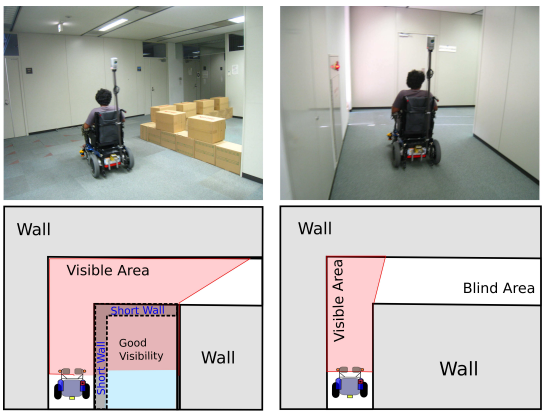

Fig. 1. Wheelchair turning right in a corner. In both cases the person faces similar traversable characteristics, however, the visibility characteristics (in red) are different. In the left image the passenger is aware of what to expect after turning while in the right, the passenger does not know what to expect after turning the corner

Previous work [1] presented an approach to build a Human-Comfort Factor Map ("HCoM") which allows a planner to compute comfortable paths. The limitation of the work is that the approach can only be extended to model straight path environments. In this work we extend the study and include the modeling of turns. We propose to compute a visibility index which could be used for computing paths for autonomous vehicles.

This paper introduces a study with human participants who manually drove the wheelchair in an indoor loop environment. Based on this study we extracted human tendencies for approaching blind and non-blind turns. Then, the same participants rode the wheelchair in autonomous mode and pressed a button given to them in the case they felt discomfort or stress. We present a discussion of the correlation between environmental visibility and navigational comfort.

A. Comfort

Previous works addressed human comfort oriented towards seat ergonomics [2] where subjective and objective methods to measure comfort were discussed. Subjective methods (asking people how comfortable they are) are direct, whereas objective methods (electromyography or stress measurements)

are indirect but less time consuming and less prone to error. Nevertheless, it is difficult to measure the origin of the measurements obtained. In other works, vehicle comfort factors were classified into dynamic (vibrations, shocks), ambient (thermal, noise) and ergonomics (passenger's position) [3]. In [4], vehicle ride comfort is measured objectively considering mechanical vibration, shock and jerk as one of the main source of discomfort.

In this work we study the relation between vehicle ride discomfort and environment visibility. Discomfort was extracted directly asking humans to press a button. We argue that visibility, which depends on the surrounding characteristics, plays an important role in the navigational style of humans and conclude that if environment visibility from the present location is not modeled, then, comfortable navigation is not feasible. This assertion is discussed in the evaluation section and throughout the paper.

B. Visibility Concept in Mapping and Robot Systems

There are previous works related to visibility modeling. Chown et al. [5] defined the term gateway to refer to the locations with major changes in visibility, where there is visual separation between neighboring areas. Occlusion finding using virtual line models on laser sensor data to find gateways was proposed in [6]. In cognitive robot mapping, gateways were also used as the directional places which separate environments [7]. In the work presented in this paper, we modeled the visibility of the passenger as centered on the seat of the wheelchair. and human comfort while driving a wheelchair. We argue about the existing correlation between environment visibility and human navigational comfort.

C. Wheelchair Navigation

Robotic wheelchairs provide users with mobility autonomy and safe navigation [8] and have been product of previous research [9], [10], [11]. In these previous works, the visibility model of the passenger was not specifically modeled and related to the navigational style. Human-wheelchair collaboration works have been presented in the literature. A system to detect user's needs and intentions using multiple hypotheses method and dynamically generating safe trajectories was proposed in [12]. Wang J. et al., in [13] proposed to adapt a wheelchair assistance to variations of user performance and environmental changes evaluating safety, comfort (comfort is measured as function of the jerk of the vehicle) and obedience in real time. Vander Poorten et al., in [14] proposed a haptic guidance algorithm to provide assistance for electric wheelchair navigation through narrow spaces. Differently to the previous works on wheelchair navigation assistance, the main point in the approach presented in this paper is the modeling of visibility for safe comfortable navigation.

In our experiments we present an analysis of 30 different wheelchair participants in an indoor corridor loop environment containing a couple of blind corners and a couple of corners with good visibility. Experimental results show moderate correlation between the visibility characteristics of the environment and discomfort of the participants.

II. Visibility Modeling

The visibility model is composed of three main parts: a robotic wheelchair, $3D$ data information and an environment representation. The output is a *visibility index* which is an indicator of the visible traversable areas in the environment from the point of view of the robotic wheelchair.

In the rest of the section the $3D$ field of view of the robotic wheelchair is explained, then, the two-layered environment representation is presented. Finally, the approach to combine the field of view with the environmental representation to compute the visibility index is detailed.

A. Field of View

Human eye visual field extends beyond 90 degrees in the transverse direction; this is the field where something can be seen. With both of the eyes the horizontal field can be extended up to 200^o [15]. In this work, the field of view was modeled as a field of 180^o horizontal and 20^o vertical. The range data coming from an omnidirectional $3D$ laser sensor was used to model the field of view and only the data within the aforementioned thresholds was used. The range was limited to $r_{Max} = 8\ m$ which we found a reasonable distance corresponding to 5 seconds ahead of the position of the wheelchair at its maximum velocity of 1.6 m/sec. For reference see Figure 2.

The reason to select a vertical field of view of 20^o was to avoid laser hits corresponding to the roof or the floor. As the wheelchair localization module has inaccuracies where a small drift in angle would produce a big error as distance increases, the range distance was thresholded.

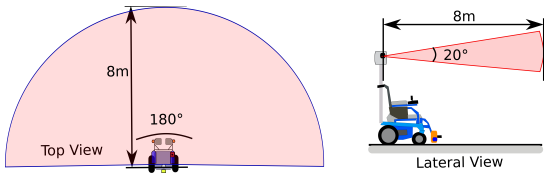

Fig. 2. $3D$ field of view of the wheelchair. Visibility is modeled as 180^o horizontal and 20^o vertical.

The field of view is attached to the wheelchair and moves and turns with it. It is projected on the environmental model to compute the visible and non-visible areas of the environment.

B. Environment Representation

The environment model has two layers. One layer contains the three-dimensional occupancy voxel map and the other one contains the traversable areas of it. The $3D$ voxel map provides the framework to perform ray-casting with the laser sensor and the $2D$ occupancy grid map to provide the traversable areas in the environment. Overall, this representation allows to differentiate between visible areas from traversable areas and their combinations (Figs. 1, 4 and 6) .

C. Visibility Index Computation

The visibility index V_{index} is a number from 0 to 1 that represents the ratio of ray-casted laser beams that are traversable and visible. The index is a function $f(r_i, m) = [0,1]$ of all the i^{th} laser beams r_i within the field of view that are projected into the environmental map m. The ratio reaches its maximum if all the traversable areas within the field of view are visible; the ratio reaches its minimum when the traversable areas are not within the visible area. A ray-casting technique is applied on every laser beam of the field of view towards the environmental model. The visibility analysis is summarized in Fig. 3 and the process is detailed below:

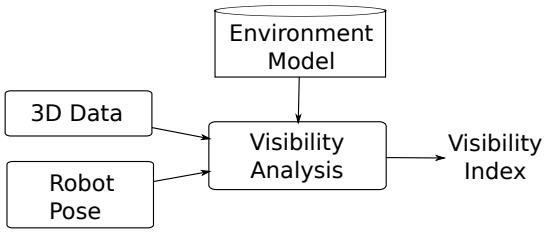

Fig. 3. Visibility analysis block diagram. The inputs of the model are the robot pose, $3D$ visibility data information and the geometric representation. The output is the visibility index.

Starting from the origin r_{Or}, the ray is casted until its maximum range r_{Max}; depending on the region in which each ray segment falls it is classified in one of four categories (Fig. 4):

1) Visible and traversable (green in Figs. 4(a) to 4(d)): the ray goes from r_{Or} to r_{Max} without any hit.
2) Visible but not traversable (green in top of Figs. 4(c) and 4(d)): the ray may hit or not hit a wall but falls in a non-traversable region.
3) Not visible but traversable (red in Figs. 4(a) to 4(d)): the ray starts from a previous hit $r_{Hit_{-1}}$ and ends in another hit r_{Hit} or the max range r_{Max} and is located on a traversable region.
4) Not visible and non traversable (yellow in Figs. 4(a), 4(b)): the ray starts from a previous hit $r_{Hit_{-1}}$ and ends in another hit r_{Hit} or the max range r_{Max} and is located on a non-traversable region.

Finally the visibility index V_{index} is given by

$$V_{index} = \frac{R_{VT}}{R_{VT} + R_{NT}} \tag{1}$$

where $R_{VT} = \sum^{k} S_{VT\,k}$ is the sum of the length of all the k visible and traversable laser ray segments S_{VT} and $R_{NT} = \sum^{j} S_{NT\,j}$ is the sum of all non-visible but traversable j segments S_{NT}. As shown in experimental results, the proposed index is capable to model good visibility corners from blind corners. Moreover, it properly models intersections according to the direction of travel (Fig. 8).

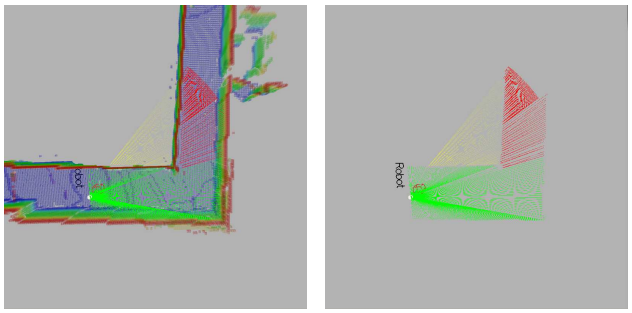

(a) Visibility region in blind corner. (b) Visibility region in blind corner.

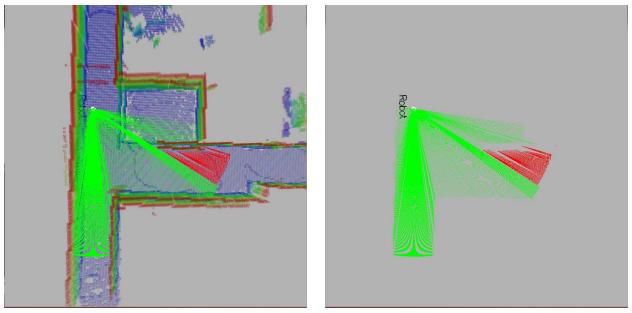

(c) Visibility in non-blind corner. (d) Visibility in non-blind corner.

Fig. 4. Visibility analysis on a blind corner on the top and a good visibility corner on the bottom. The visible ray segments are shown in green, the non-visible but traversable are in red and the non-visible and non-traversable are in yellow. The figure presents snapshots of our data viewer (in OpenGL) showing real experiment data.

III. System Overview and Implementation

A. Robotic Wheelchair and Sensor Framework

Experiments were conducted using an electric wheelchair from Imasen Engineering Corporation. The wheelchair could be controlled with a joystick and at the same time it is interfaced with a laptop computer using USB communication. The wheel encoder data was received by the program on the laptop and velocity commands could be sent to the wheelchair. All the software used for controlling the wheelchair motion was executed on this laptop computer. The wheelchair was equipped with a Velodyne $HDL-32E$ laser scanner, two Hokuyo $UTM-30LX$ $2D$ laser scanners and a Crossbow $VG440$ Inertial Measurement Unit (IMU). The placement of the sensors is shown in Fig 5.

B. Building the Environment Model

The maps were built off-line with logged data. The building process is briefly explained below.

1) 3D Map Building: The robotic wheelchair is equipped with wheel encoders which were used to obtain odometry data and a velodyne laser sensor was used to obtain the range information. To build the map, we drove the wheelchair with the joystick while the odometry and the laser sensor information were recorded. We used an iterative closest point (ICP) based SLAM to correct the trajectory of the robot and align the laser sensor scans using the $3DToolkit$ library framework [16]. After obtaining the point cloud map, we down-sampled into $3D$ voxels ordered in an octree structure

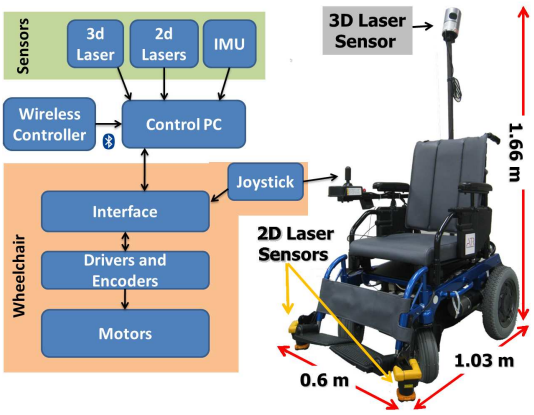

Fig. 5. Robotic wheelchair equipped with a 3*D* laser sensor, two 2*D* laser sensors, an IMU, a bluetooth controller and wheel encoders.

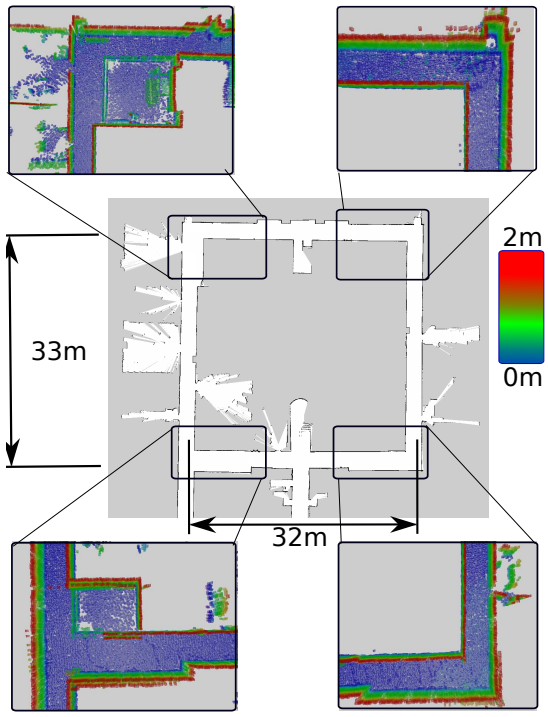

Fig. 6. Environment representation. The occupancy grid map is in the center where traversable areas are in white and non-traversable areas are in black and gray. The corners of the 3*D* map are shown where the coloring represents the different height of the voxels. The corners on the left have good visibility and the ones on the right have poor visibility.

using the octomap library framework of [17] where the voxel resolution was set to $0.1m \times 0.1m \times 0.1m$.

2) 2D Map Building: The occupancy grid map was built using the gmapping framework from the robot operative system (ROS) [18]. The map is shown in Fig. 6 and share the same coordinate frame as the 3*D* map. The field of view was combined with the occupancy grid map to perform a check of the traversable areas that are present. Traversable areas are the free cell areas (in white) and the non traversable areas are the occupied cells and the unknown cells (black and gray).

C. Wheelchair Localization

The wheelchair localizes itself towards the map using a particle filter approach based on laser data ray-casting [19]. Each particle contains a pose given by state vector $\hat{x} = \{x, y, \theta\}$, with position x and y and orientation θ.

IV. Human Comfort Extraction

In this work we assume that comfortable navigation is achieved when the user of the wheelchair does not feel in danger or stressed, i.e., not in discomfort. Hence, we extract the time stamped locations where participants felt stressed, uneasy or in discomfort. The objective of the experiment was to extract discomfort under the following conditions:

- All participants have used the wheelchair: before the experiment, participants were allowed to practice and drive the wheelchair.
- Participant discomfort was extracted while they rode the wheelchair during autonomous navigation:
  - Through a couple of the participant's own replayed trajectories without knowledge of it.
  - Through a couple of trajectories from an expert driver (common to all participants). The expert drove the wheelchair with few zig-zag effects and velocities close to maximum.
- During navigation participants were provided a wireless button which they pressed in case of feeling in discomfort or danger.

A. Experimental Procedure

We called 30 Japanese people with an average age of 21.5 years (15 females and 15 males) who were payed for their participation and did not have knowledge of the content or objective of the experiments. The experiment was held in an indoor corridor environment with four corners, two with poor visibility (Fig. 6 top and bottom right) and two with good visibility (Fig. 6 top and bottom left). The total length of the path was of approximately 130 *m*. The experiments were divided in two phases: self driving and autonomous ride, where participants traversed the environment the same amount of time clockwise and counter-clockwise (CW/CCW). We recorded all the time stamped positions, linear/angular velocities, accelerations, laser data and stress button control (only for autonomous navigation). The experiments had three steps:

1) Getting familiar with the wheelchair: Before starting the experiment, each participant was asked to drive the wheelchair in an empty room for some minutes in order to get used to the wheelchair control. Once they felt comfortable with the joystick control, they were asked to drive the wheelchair in the corridor loop shown in Fig. 6.

2) Manual Driving: Each participant drove the wheelchair manually in the corridor making 8 loops (4 CW + 4 CCW). They drove at their own comfortable driving style and velocities. The path of the wheelchair during their manual control was recorded.

3) Autonomous Driving: Participants were asked to sit on the wheelchair while it navigated autonomously replaying two of the trajectories (CW and CCW) they followed during the last lap of their manual driving and two of the trajectories (CW and CCW) recorded by an expert who drove at high velocities and few jerking. The order of the four different autonomous runs were jumbled for all participants.

B. Extracting Comfort Information

In order to obtain the subjective feedback from the participants about the comfort on the wheelchair navigation, they were given a wireless controller and were asked to press a button whenever they felt it as uncomfortable or uneasy. We performed an analysis of the places in which participants were pressing the controller and related it with different discomfort effects:

- Poor visibility of the environment (blind corners or intersections).
- Zig-zag effects are known to have effect in navigational comfort [4] and are out of the scope of this work.

V. Evaluation and Discussion

This section presents an evaluation of the proposed visibility analysis in the four corner regions of the experimental environment of Fig. 6. The histogram of the number of observations of a specific visibility index and the histogram of the number of button clicks are presented. Then their relation is discussed. We computed the correlation coefficient between discomfort (stress button clicks) and visibility index value. Then experimental results show the difference of the visibility index when driving CW and CCW. Finally we discuss the system limitations.

A. Correlation between visibility and discomfort

Using the data of the 30 participants while riding the wheelchair autonomously (four runs per participant) we built the histograms of Figure 7 which show the relation between the visibility index and the number of times that the stress button was pressed. The visibility index is shown on the horizontal axis of the histograms in a range from 0 to 1 divided in 50 bins (0.02 per bin). The top histogram shows the total number of observations ($N_{Observation}$) of a determined visibility index. The middle histogram shows the total number of times in which the passengers pressed the button (N_{Button}) when they felt stress or discomfort. In the bottom histogram, the vertical axis shows the visibility-observation ratio (R) of the number of times that the stress button was pressed in each bin divided by the total number of observations. The visibility-observation ratio for the i^{th} bin is given by expression (2):

$$Ratio = \frac{N_{Button}}{N_{Observation}} \tag{2}$$

Figure 7 shows that the histogram had a maximum ratio value R_i at $V_{index} = 0.6$ and as V_{index} increases the ratio values decreased. In these experiments, the wheelchair kept enough distance from the wall and obstacles, therefore, the visibility index became bigger than 0.6. The Pearsons correlation coefficient of the *Ratio* value and the visibility index is -0.627 ($p = 0.002$). This can be interpreted as the participants feeling less comfortable at lower values of visibility. As V_{index} increased the rate in which participants pressed the button decreased as the visibility was better.

For our experimental data set, as the results in Fig. 7 show, at low visibility the ratio reaches its maximal value 1. It is expected to have higher ratio as V_{index} decreases, however, reaching the maximal value is not expected if similar experiments are held with a different data set.

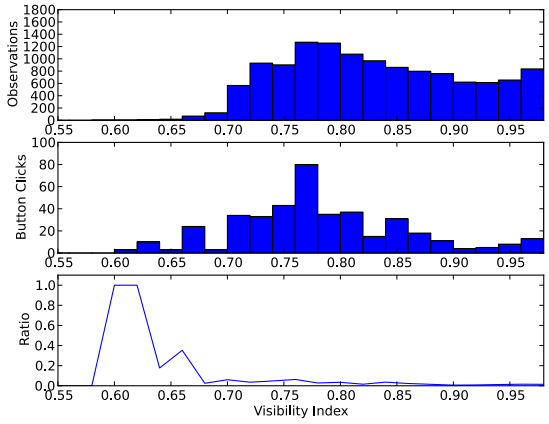

Fig. 7. Environment visibility histograms where the horizontal represents the visibility index in a range from 0 1 divided in 50 bins. The top shows the histogram with the total number of observations $N_{Observation}$. In the middle the total number of times in which the button was pressed N_{Button}. The bottom shows the visibility-observation ratio (R) .

B. Visibility modeling

The approach presented in this work is capable of modeling environmental visibility according to the direction of motion. Results of visibility index while driving CW and CCW are shown in Figs. 8(a) and 8(b). It is notable that in the corner at the bottom right of Figs. 8(a) and 8(b) the visibility index score when going CW is very low as the corridor coming from the right is not visible, on the contrary, when going CCW the corridors coming from the top and right are visible, therefore the visibility score is high.

Fig. 9 (left) shows how people driving in blind corners tend to "over" turn in order to gain visibility while turning. On the contrary, Fig. 9 (right) shows how in non-blind corners (good visibility like Fig. 1 left side) the participant drove even closer to the corner.

C. Discussion

The visibility index is a value between 0 and 1, however, results show that for our environment values under 0.5 were not found. In other types of environments lower values could be computed, therefore we decided not to shift the index to the left (Fig. 7). As our experimental environment was simple there was no need to perform a connectivity analysis (e.g., using a topological map) to compute what next possible paths are traversable in the case of intersections.

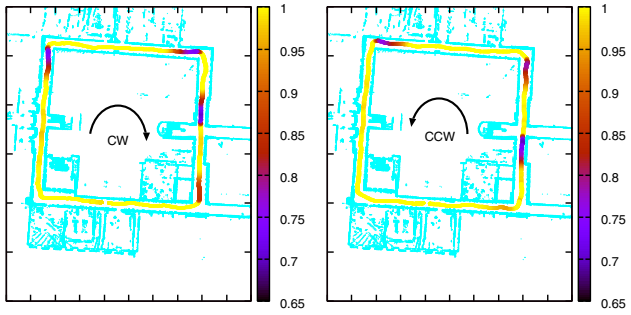

(a) Running clockwise. (b) Running counter clockwise.

Fig. 8. Visibility index in a robotic wheelchair run. It can be appreciated how the visibility is modeled differently when running clockwise than that counter-clock wise. This is more noticeable at the bottom right of the graphs.

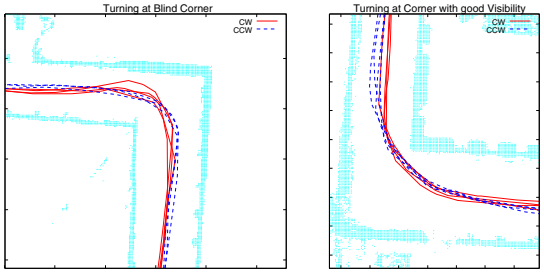

Fig. 9. Trajectories of a participant driving the wheelchair clockwise (CW) and counter clockwise (CCW). It can be seen how people try to increase the visibility while turning in the blind corners.

Experimental results did not offer evidence of difference in discomfort between driving CW or CCW. Also no conclusive difference between expert and self driving runs was found. We believe that passengers get habituated to the navigation of the vehicle after few runs; this is, the more experienced they become the less stressed they feel. Passenger habituation effects during navigation need to be observed and modeled.It is left for future work to study habituation effects in the correlation coefficient between stress and visibility index.

In this work we used a robotic wheelchair as experimental platform and did not perform experiments with real wheelchair users. This work is not intended to be vehicle specific and its results should be useful for other types of personal mobility devices.

VI. Conclusions

This paper presented a novel approach for modeling the visibility of a passenger on a vehicle. Experimental results show that human participant discomfort during navigation in corners has moderate correlation to environmental visibility. The visibility analysis presented in this work can differentiate between corners with same traversable characteristics but different visibility (corners in Fig. 8). Furthermore, results confirm that the proposed approach offers different visibility index at the same location of the environment depending on the driving direction (bottom left corner of Figs. 8 (a) and (b)). As future work we plan the implementation of a path planner which uses the visibility index as a parameter to compute comfortable paths according to the characteristics of the environment. We are working in the integration of the visibility model to a human comfort map (HCoM)[1] to compute human comfortable paths based on the environmental visibility in turns, corners and intersections.

References

[1] Y. Morales, N. Kallakuri, K. Shinozawa, T. Miyashita, and N. Hagita, "Human-comfortable navigation for an autonomous robotic wheelchair," in *Intelligent Robots and Systems (IROS), 2013 IEEE/RSJ International Conference on*, 2013.

[2] M. de Looze, L. Kuijt-Evers, and J. van Dien, "Sitting comfort and discomfort and the relationships with objective measures." *Ergonomics*, vol. 46, no. 10, pp. 985–97, 2003.

[3] O. Ormu, Krunoslav; Mufti, "Main ambient factors influencing passenger vehicle comfort," *Proceedings of 2nd International Ergonomics Conference*, vol. 2, pp. 77–84, 2004.

[4] K. Strandemar and K. tekniska högskolan, *On Objective Measures for Ride Comfort Evaluation*, ser. Trita-S3-REG, 2005. [Online]. Available: http://books.google.co.jp/books?id=loectgAACAAJ

[5] E. Chown, S. Kaplan, and D. Kortenkamp, "Prototypes, location, and associative networks (plan): Towards a unified theory of cognitive mapping," *Cognitive Science*, vol. 19, no. 1, pp. 1–51, 1995.

[6] D. Schröter, T. Weber, M. Beetz, and B. Radig, "Detection and classification of gateways for the acquisition of structured robot maps," in *DAGM-Symposium*, 2004, pp. 553–561.

[7] P. Beeson, J. Modayil, and B. Kuipers, "Factoring the mapping problem: Mobile robot map-building in the Hybrid Spatial Semantic Hierarchy," *International Journal of Robotics Research*, vol. 29, no. 4, pp. 428–459, 2010.

[8] E. Wästlund, K. Sponseller, and O. Pettersson, "What you see is where you go: testing a gaze-driven power wheelchair for individuals with severe multiple disabilities," in *Proceedings of the 2010 Symposium on Eye-Tracking Research Applications*. New York, NY, USA: ACM, 2010, pp. 133–136.

[9] E. Prassler, D. Bank, and B. Kluge, "Key technologies in robot assistants: Motion coordination between a human and a mobile robot," *Transactions on Control, Automation and Systems Engineering*, vol. 4, 2002.

[10] Y. Kobayashi, Y. Kinpara, T. Shibusawa, and Y. Kuno, "Robotic wheelchair based on observations of people using integrated sensors," in *Intelligent Robots and Systems, 2009. IROS 2009. IEEE/RSJ International Conference on*, oct. 2009, pp. 2013 –2018.

[11] A. Argyros, P. Georgiadis, P. Trahanias, and D. P. Tsakiris, "Semi-autonomous navigation of a robotic wheelchair," *Journal of Intelligent and Robotic Systems*, vol. 34, 2001.

[12] T. Carlson and Y. Demiris, "Human-wheelchair collaboration through prediction of intention and adaptive assistance," in *in Proc. of IEEE International Conference on Robotics and Automation*, 2008, pp. 3926–3931.

[13] Q. Li, W. Chen, and J. Wang, "Dynamic shared control for human-wheelchair cooperation," in *Robotics and Automation (ICRA), 2011 IEEE International Conference on*, 2011, pp. 4278–4283.

[14] E. Vander Poorten, E. Demeester, E. Reekmans, J. Philips, A. Huntemann, and J. De Schutter, "Powered wheelchair navigation assistance through kinematically correct environmental haptic feedback," in *Robotics and Automation (ICRA), 2012 IEEE International Conference on*, 2012, pp. 3706–3712.

[15] D. Henson, *Visual fields, 2nd edition*. Butterworth-Heinemann, 2000.

[16] A. Nuchter, K. Lingemann, J. Hertzberg, and H. Surmann, "6d slam-3d mapping outdoor environments." *Journal of Field Robotics*, vol. 24, no. 8-9, pp. 699–722, August 2007.

[17] A. Hornung, K. M. Wurm, M. Bennewitz, C. Stachniss, and W. Burgard, "OctoMap: An efficient probabilistic 3D mapping framework based on octrees," *Autonomous Robots*, 2013, software available at http://octomap.github.com. [Online]. Available: http://octomap.github.com

[18] G. Grisetti, C. Stachniss, and W. Burgard, "Improved techniques for grid mapping with rao-blackwellized particle filters," *Robotics, IEEE Transactions on*, vol. 23, no. 1, pp. 34–46, 2007.

[19] F. Dellaert, D. Fox, W. Burgard, and S. Thrun, "Monte carlo localization for mobile robots," in *IEEE International Conference on Robotics and Automation (ICRA99)*, May 1999.